Science Advances
AAAS
Manuscript Template

FRONT MATTERS

Understanding deep ultraviolet surface enhanced Raman scattering: case study of Pt nanoparticles with modified Work Functions

Authors

Barbara F. Scremin,[1,*] Francesco D'Amico[2], Cinzia Cepek[1], Alberto Morgante[1,3], Moreno Meneghetti[4,*]

Affiliations

[1] CNR – Material Foundry Institute (IOM), AREA Science Park, Strada Statale 14 Km 163.5, 34149 Trieste, Italy.

[2] Elettra Trieste Synchrotron, S.S. 114 km 163, Basovizza, 34149 Trieste, Italy.

[3] Physics Department, University of Trieste, Via Valerio 2, Trieste, 34127, Italy.

[4] Chemical Sciences Department, University of Padova, Via Marzolo, 1, 35131, Padova, Italy.

[*]scremin@iom.cnr.it, moreno.meneghetti@unipd.it

Abstract

Deep ultraviolet surface enhanced Raman scattering (DUV SERS) spectra were on the focus of many works in the past two decades promising strong Raman signals from biological molecules. However, although the high potential, unexpectedly, results were poor. Pt nanoparticles with a plasmon band in the deep UV (DUV) were taken here as model system. Extinctions spectra were calculated for the interpretation of the plasmon band, together with input electromagnetic field enhancement factors for the interpretation of SERS experimental results. Experiments and computations based on ellipsometry experimental literature data evidenced that the metal nanoparticles work function (WF) affected the intensity SERS bands of a test biological molecule on metal surface. DUV SERS signals dependence on metal WF was evidenced by tuning it by surface modification with sodium, chlorine and fluorine atoms. Obtained results show for the first time how WF works as a critical parameter for metal substrates in DUV SERS.

Teaser

Metal nanoparticles work functions in the deep ultraviolet excitation region: tuning and effects on surface enhanced Raman spectra of a biological molecule on their metal surface.

Introduction

Obtaining the deep ultraviolet surface enhanced Raman scattering (DUV SERS), with excitation below 300 nm (4.13 eV), is a goal that researchers have been pursuing in the past 20 years for obtaining intense Raman spectra of molecules in traces at the surface of nanostructured suitable metals (1-6). In the UV region the intensity of the Raman scattering is increased because of its fourth power frequency dependence and because of possible resonance conditions, in particular for biological molecules. SERS, may increase the Raman scattering signals by many orders of magnitude.

The SERS effect is related to the localized surface plasmon resonances (LSPR) of nanostructured materials, in particular of metals which display a negative real part of the dielectric function below the plasmon frequency. This is a property of the metal dielectric function, and is mandatory for the fulfilment of the so called Fröhlich condition, at the base of the electromagnetic exciting field enhancement by the nanostructured metal (7-8).

Several metals, like for example Al, Rh, Pt, Pd, have been considered for DUV SERS, because they are predicted to have plasmon resonances in the required DUV energy range, but the experimental literature results did not show the expected SERS enhancements, in particular if a comparison is made with the results recorded with nanostructured materials based on Ag and Au (noble metals) excited in the visible and near infrared. For Au studies single molecule SERS was also obtained (8). Al nanoparticles have been the most studied material for DUV SERS, but it has been recognized that the formation of some nm of passivating oxide (Al_2O_3) on their surface reduce the SERS enhancement factor (9), shifting the plasmon peak towards the visible (10). Alternatively, Pt nanoparticles do not passivate with oxygen at the surface (Fig. S4) as Al ones, then possibly generate SERS in the DUV. Pt is a very stable noble metal, an important characteristic for nanosystems used in ‘complex and reactive’ environments like those found in biological applications. Pt nanoparticles show a localized plasmon resonance in DUV, but very few results, and with poor SERS enhancements, have been reported in the literature in the UV (11) and DUV (12) energy ranges. On the other side, SERS results have been reported with excitation of Pt nanoparticles in the visible and NIR regions (13), then these experiments did not exploit the properties which would make these nanoparticles interesting for DUV SERS.

Here we report calculations and experiments for exploiting the DUV SERS properties of Pt nanostructures.

Pt nanoparticles were produced by laser ablation in water (15), a physical method which is one of the cleanest synthetic approaches for

obtaining nanoparticles with naked surfaces, mandatory for the subsequent functionalization with molecules under SERS investigation, with applications like targeting of tumor cells antigens, now days common with gold nanoparticles (AuNP) (16-20). Past literature results with AuNP particularly were a guide for understanding the SERS properties of Pt nanoparticles with electrodynamic Mie calculations performed using boundary elements methods (BEM) (21, 22). Experiments on the other side showed the importance of the work function (WF) of the metal nanostructures, never considered before the present research study for DUV SERS experiments, and WF fundamental role in determining the overall DUV SERS efficiency. In fact, unlike conventional SERS performed with visible or NIR excitation sources, the DUV photons may have sufficient energy to extract electrons from the nanoparticles. These electrons can modify the surface bounded molecules, which determine the DUV SERS spectrum. In order to shed light on this process, we synthesized different types of Pt nanoparticles with different WF. It will be shown that WF is a fundamental parameter for obtaining the SERS spectrum of a molecule, here adenine, exciting Pt nanoparticles with photons at 266 nm (4.66 eV).

Results

Calculations for the prediction of LSPR energy and the DUV SERS enhancement factors of PtNP

First of all, the extinction (absorption + scattering) spectrum of isolated spherical Pt nanoparticles (PtNP) in water with diameters ranging from 10 to 50 nm have been calculated to identify the presence in DUV of a LSPR, mandatory to have the exciting field enhancement effect for obtaining at least in principle DUV SERS. The simulations used experimental ellipsometry data for the permittivity (or dielectric function) of fcc (face centered cubic) Pt produced by sputtering methods by Tselin et al. (23), chosen after testing other literature datasets (26). The computational technique to solve the Maxwell equations for metal nanoparticles immersed in a dielectric (the Mie problem) is the boundary element method (BEM) approach (21) with the Matlab routines implemented by Hohenester et al. (22). The results are shown in Fig.1.

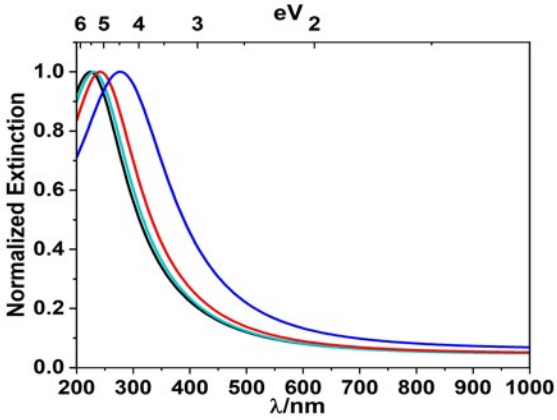

Fig. 1. Calculated PtNPs extinction (absorption + scattering) spectra in water medium. NPs size goes from 10 nm to 50 nm. Black line:10 nm, green line: 20 nm, red line: 30 nm, blue line: 50 nm. Spectra are normalized to their peak intensities. Peaks maxima of the LSPR, localized surface plasmon resonance, are reported in Table 1, red shifts from 225 nm (5.51 eV) for the smaller particle to 280 nm (4.43 eV) for the bigger one (50 nm). The contribution of interband transitions may be present (23, 27), although not evident.

PtNPs diameters	Peak Wavelength (nm, (eV))	Largest SERS enhancement factor at 266 nm (4.66 eV)
10	225 (5.51)	5.5
20	230 (5.39)	4.7
30	240 (5.16)	4.7
50	280 (4.43)	0.2

Table 1. Calculated peak wavelengths (energies) of LSPR and largest electromagnetic field SERS enhancements factors. The calculus takes into consideration PtNPs of diameters range 10-50 nm in water medium. The relative SERS enhancement factor is obtained as $(|E_{loc}(\omega_0)|/|E_0(\omega_0)|)^4$, where E_{loc} is the local electric field on the surface of the PtNPs and E_0 is the applied electric field here at ω_0=266 nm (4.66 eV).

Electromagnetic field SERS enhancement factors are presented as the fourth power of the ratio of the local field over the incident field ($|E_{loc}(\omega_0)|/|E_0(\omega_0)|)^4$ at 266 nm (4.66 eV), the photons used for the DUV SERS experiments. It is known that this amplification of the incident field is the larger contribution to SERS, being of minor importance the chemical contribution deriving from the interaction of molecules with the nanoparticle surface (27). For the isolated nanoparticle surface, where the largest electromagnetic field enhancement values can be calculated, we found very small enhancements factors: less than 10 for all the different particle sizes examined, which are reasonably resembling the experimental ones (Table 2).

It is well documented that notable enhancement factors, useful for observing SERS in experiments, are obtained within the so called “hot spots” (28), which are, usually, the small contact regions between nanoparticles or between nanoparticles and surfaces. The LSPR of hot spots can be observed in the extinction spectra of dimers of plasmonic nanoparticles. It is known, for example, that the AuNP hot spots exhibit clear dipole moment LSPR with extinction maxima in the NIR

region, from 600 nm to 900 nm and beyond, while the localized surface plasmon resonance of isolated nanoparticles is at 520 nm. These dipolar resonances depend on the size and number of aggregated nanoparticles, as it was clearly shown for AuNPs (28).

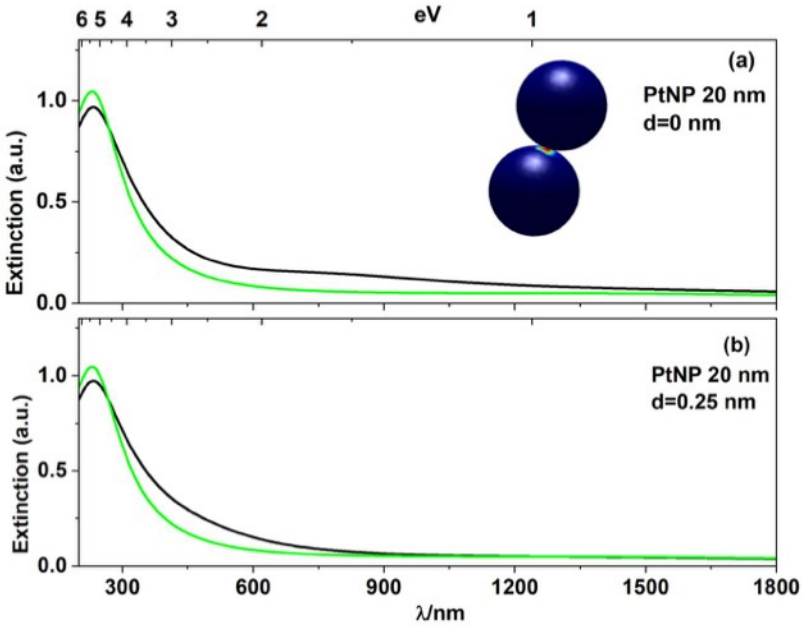

Fig. 2. Calculated extinction spectra for two PtNPs at different mutual distance in water medium vs two isolated PtNPs. (A) Black line: extinction spectrum of a dimer of PtNP of 20 nm in diameter in contact (d = 0) and green line: two isolated PtNPs. **(B)** Dimer interparticle distance d = 0.25 nm. In the inset of **(A)** example of dimer and its hotspot at the contact point of the two particles obtained in the calculation of the enhancement factors at 266 nm. Color intensity scale goes from red (maximum) to blue (minimum).

The dimer extinction spectrum of 20 nm particles of Pt in full contact (interparticle distance d=0 nm), is reported in Figure 2(A) (black line), together with the spectrum of two isolated particles (green line) for unpolarized light, as it is appropriate for particles in solution. Polarized input field along the major axis of the dimer however, from the calculations contributes essentially to the “hot spot”. With this dimer the extinction spectrum presents a new more intense shoulder toward the visible respect to the isolated PtNPs (Fig. 2(A) maximum at about 790 nm, 1.57 eV). This is the fingerprint of the localized surface plasmon resonance of the hotspot between the two particles. The increase of the extinction is observed, as in the case of AuNP, at larger wavelengths than the resonance for the isolated particles, but with much less intensity for PtNPs than for AuNPs, suggesting that the coupling of excitations of the two particles is less efficient for Pt than for Au. This could derive from the presence, for Pt, of interband transitions in this spectral region (23, 27). Increasing the distance between the particles of the dimer to 0.25 nm, one observes the shift of the resonance to higher energies (at about 530 nm, 2.34 eV, see Figure 2(B)). However, comparison with the extinction spectra of the isolated particles (see Figure 2(B)) shows that a larger extinction in

the visible is always present. Similar results were also obtained with dimers of PtNPs of 10, 30 and 50 nm (Fig. S. 5, S. 6 and S. 7).

The calculations SERS enhancement factor for the dimers at 266 nm shows an increase of several 10^3 with respects to less than 10 in the case of isolated particles. Clearly, the largest enhancements were found in the region between the nanoparticles, namely in the hot spot of the dimers (inset of Fig. 2). The amplification is not large as in the case of AuNP in the visible and NIR (28), however, an increase of some order of magnitude is found as expected for the presence of the hot spot.

PtNP diameter (nm) for NP in dimers (distance d between the NP (nm))	Largest SERS enhancement factor at 266 nm (4.66 eV)
10-10 (0)	$4.5\ 10^3$
10-10 (0.25)	$5.1\ 10^3$
20-20 (0)	$5.5\ 10^3$
20-20 (0.25)	$7.5\ 10^3$
30-30 (0)	$4.7\ 10^3$
30-30 (0.25)	$6.5\ 10^3$
50-50 (0)	$1.5\ 10^3$
50-50 (0.25)	$1.5\ 10^3$

Table 3. Largest calculated electromagnetic field SERS enhancements factors for dimers of PtNPs with excitation at 266 nm (4.66 eV). SERS enhancement factor is calculated as $((|E_{loc}(\omega_0)|/|E_0(\omega_0)|)^4$, where E_{loc} is the local electric field found in the hot spot and E_0 is the applied electric field at ω_0) for dimers of PtNPs, exciting at 266 nm (4.66 eV) in water with sizes ranging from 10 to 50 nm and interparticle distances d = 0 nm and d = 0.25 nm.

The maximum electromagnetic enhancements factors at 266 nm for the dimers of different size and with different interparticle distances (d = 0 and 0.25 nm), are reported in Table 3. One finds a larger enhancement at 266 nm (4.66 eV) for the dimer with the interparticle distance d = 0.25 nm. This can be understood observing that, increasing d, there is a shift toward the UV of the LSPR resonance of the hot spot.

One has to remember that quantum effects, in particular electron tunneling is present between metal particles when they are very close to each other, namely fraction of a nm, and new effects, usually called charge transfer plasmon resonances appear (29). These quantum effects are not included in the classical electrodynamic Mie approach, one recalls that these new resonances usually suppress the responses calculated classically (22) meaning that the presented results are upper limits of the experimentally observed enhancements.

The results of the above calculations let us concluding that, although the LSPR for PtNPs hot spots is present, the enhancement for the DUV SERS at 266 nm, is smaller than usually found for AuNP in the visible and NIR. However, to confirm these conclusions we performed DUV SERS experiments with PtNPs using one of the most used standard molecules for such a measurement i.e. adenine.

DUV-SERS of adenine with different PtNPs

PtNPs with naked surfaces from laser ablation of a Pt target in double distilled water were obtained using ns pulses at 1064 nm (Materials and Methods) produced good hot spots in which the distance between the particles approaches d = 0.

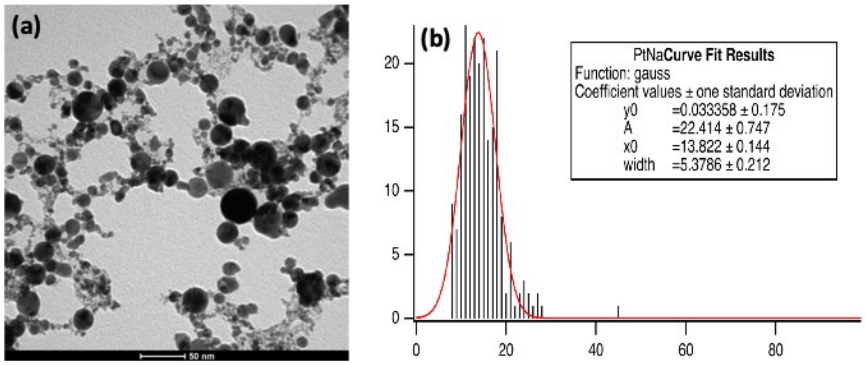

Fig. 3. Morphology and size distribution of Pt NPs. (A) TEM image of the PtNPs obtained by ablation laser synthesis with 9 ns pulses at 1064 nm of Pt bulk target under double distilled water; **(B)** PtNPs size distribution histogram and its gaussian fitting.

A TEM image of the synthesized PtNPs is shown in Fig. 3 (A), together with their size distribution in Fig. 3 (B). The gaussian fitting shows that the average size is 14 nm with a width of 5 nm. All the peaks observed with XRD can be indexed with the face cantered cubic structure of Pt (Fig. S1).

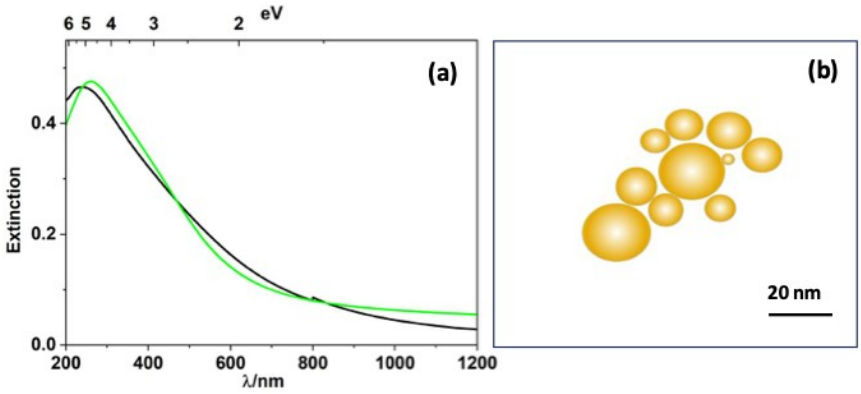

Fig. 4. Experimental and calculated extinction spectra of aggregated PtNps. (A) Black line: experimental extinction spectrum of the PtNPs synthesized by laser ablation of a bulk Pt target under double distilled water; green line: BEM calculated extinction spectrum for a model aggregate of Pt NPs in water reported in (B). **(B)** Model of aggregated PtNPs, inspired TEM images, used for the calculation of the extinction spectrum in (A)-green line.

The UV-vis-NIR extinction spectrum of the water solution of PtNPs is reported in Figure 4a (black line). A maximum is present at 240 nm and can be interpreted as the LSPR of the PtNP. According to the

above calculations, the presence of a broad 'shoulder' at larger wavelengths shows that the particles are aggregated in solution.

The calculated extinction spectrum of a cluster of 11 PtNPs in solution (Fig. 4b), inspired by TEM images is reported in Figure 4a (green line). The experimental spectrum is well reproduced, in spite of the low number of particles considered. A bigger cluster containing the 70 NPs of the selected TEM image run out of available calculation memory. Calculated DUV SERS excited at 266 nm (4.66 eV), which was 2.2 10^3, in agreement with the calculations for dimers reported in Table 3.

DUV SERS experiment were performed evaporating 1 ml of the PtNP solution with extinction of 0.47 at 240 nm, on a Si surface obtaining a spot of about 5 mm of diameter. This ensured that the particles were aggregated and that hot spots were present. Over the dried PtNPs, we evaporated 1 ml of 10^{-3} M adenine solution in EtOH. However, it was not possible to register any adenine spectrum exciting at 266 nm with 0.3 mW on the sample. The Raman spectrum of 1 ml of the same adenine solution evaporated over the Si surface, without the presence of the PtNPs, is reported in Figure 5(A).

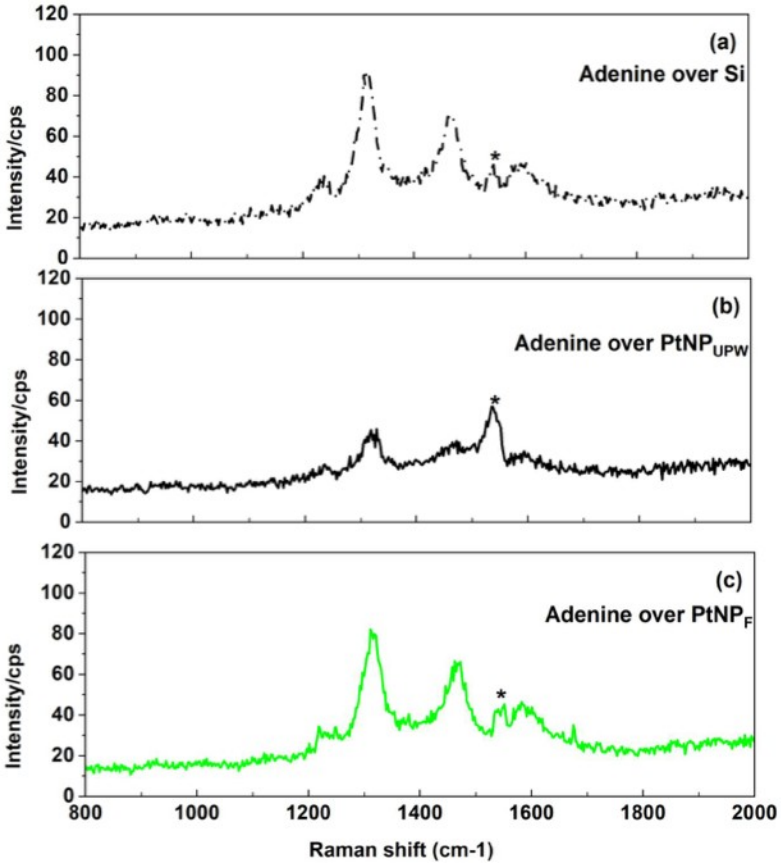

Fig. 5. Experimental DUV Raman and SERS Spectra of adenine. (A) Dashed black line: DUV Raman spectrum, excited at 266 nm (4.66 eV), of 1 ml of 10^{-3} M solution of adenine in EtOH evaporated on a Si surface. **(B)** Black line: DUV SERS for the same deposition of adenine over $PtNP_{UPW}$. **(C)** Green line: DUV SERS for the same deposition of adenine but over $PtNP_F$. The Raman band of the oxygen present in air is observed at 1555 cm^{-1} and indicated with an asterisk in the spectra.

The result shows that the presence of the PtNPs prevents recording of a spectrum of adenine, also if the calculated enhancement for the SERS spectrum excited at 266 nm (4.66 eV), although small, was explicit.

Characterization and tailoring of the surface properties of PtNPs

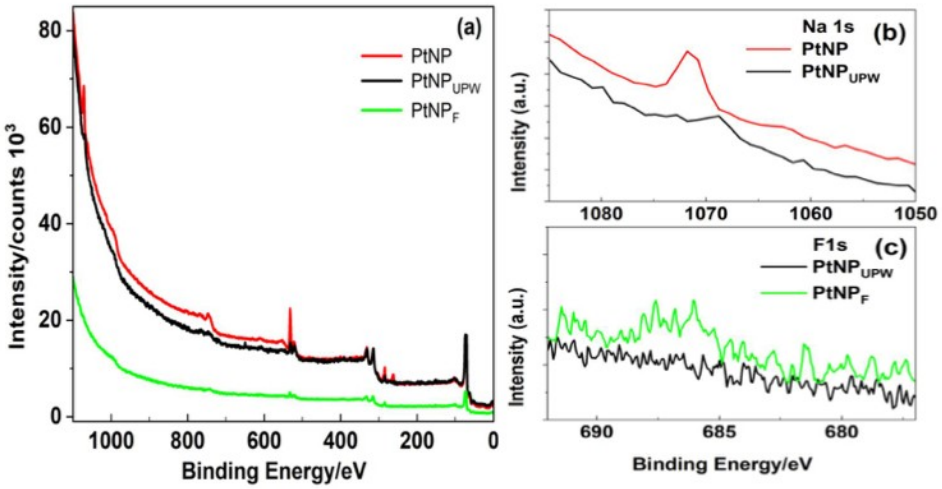

Fig. 6. XPS surface analysis. (A) Red line: XPS survey spectrum of PtNPs from Pt laser ablation in double distilled water; black line: $PtNP_{UPW}$ (in ultrapure water); green line: $PtNP_F$ (ultrapure water and F-doped); **(B)** red line: Na 1s peak at 1071 eV for PtNP; black line: $PtNP_{UPW}$; **(C)** F 1s spectral region of at 690 eV: black line: $PtNP_{UPW}$; green line: $PtNP_F$. Cross section of F is about ¼ of that of Na.

Surface properties of the first laser ablation synthesis in double distilled water named simply PtNPs were characterized first of all by recoding the XPS survey spectrum: surprisingly it was detected a Na contamination most probably from double distilled water (Figure 6 (A) red line). This "fortunate" event suggested the modification of the WF by Na atoms at the surface of PtNPs. WF modification by atoms at the surface of metals is a fact that is demonstrated in the literature from long time (31, 32). It was so decided to tune the PtNPs first of all synthesizing them in ultrapure water (zero conductivity Certipur water, materials and methods) to increase the WF, that for bulk fcc Pt is around 5 eV, then to dope the surface of these latter pure Pt NPs, named $PtNP_{UPW}$ with F to increase the WF above 5 eV (Figure. 7). We add that MilliQ water in borosilicate glass ablation cells was tested at the end and did not present appreciable Na contamination as double distilled water that was used in literature laser ablation synthesis and DUV SERS experiments most of the times, if not always.

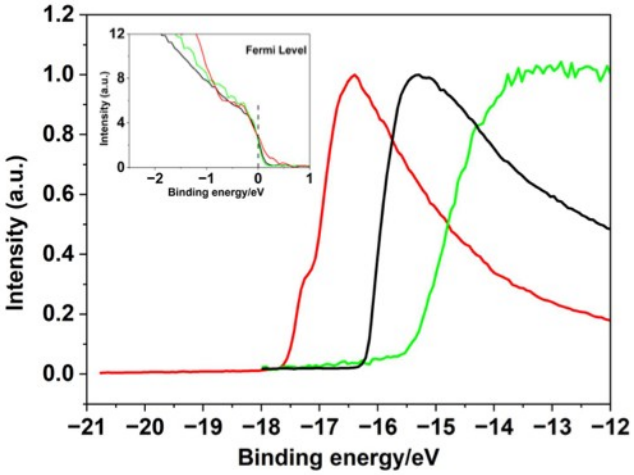

Fig. 7. UPS spectra of the Pt nanoparticles synthesized with WF tuning. Red line: PtNPs in double distilled water and synthesized in glass ablation cell; black line: $PtNP_{UPW}$ synthesized in ultra-pure water and quartz containers; green line: $PtNP_{UPW}$ doped with HF named $PtNP_F$. The inset shows the Fermi levels of the different nanoparticles presented in the main figure.

UPS measurement, consequently performed, and the results are reported in Figure 7. WF of Na contaminated PtNPs (red line) was 3.6 eV, a very low value with respect to values above 5.5 eV for a clean surface of Pt (35). This low value of the WF is of particular importance for the DUV SERS because photons have energies larger than the WF. In the present case the energy of the photons at 266 nm is 4.66 eV, well above the WF of the Na contaminated PtNPs. This suggested us that photons at 266 nm cause photoelectron emission and that these electrons can be captured by molecules of adenine deposited on PtNPs. The capture of low energy electrons was already reported for adenine (34).

The facts suggest that the failure in the registration of the spectrum of adenine deposited on PtNPs derives from the modification/destruction of the adenine molecule by the photoelectrons extracted from PtNPs. Confirmation of this conclusion can be obtained using PtNPs with WF larger than the energy of the exciting SERS photons used for the experiments. Therefore, next step in understanding these results was the synthesis of Pt nanoparticles with an increased WF by F doping.

Synthesis of PtNPs with increased WF and new DUV SERS of adenine

Containers and water used for the syntheses of the PtNPs were considered as possible sources of Na atoms doping the PtNPs, and, therefore, another synthesis was performed using ultrapure water and quartz ablation cell obtaining $PtNP_{UPW}$ (Materials and Methods). Solutions were then stored in FEP containers. TEM images of the $PtNP_{UPW}$ are reported in Fig. S2 together with the distribution of particle sizes.

The XPS spectrum of the new synthesized $PtNP_{UPW}$ showed that they were free of Na (Figure 6, black line), and with the UPS measurements (Fig. 7, black line) it was found an increase in the WF to 4.9 eV, a value now larger than the photon energy at 266 nm (4.66 eV) of the SERS exciting laser.

DUV SERS experiment at 266 nm with $PtNP_{UPW}$ with the same procedure used before with Na doped PtNPs was performed. The resulting spectrum is reported in Figure 5(B). The spectrum of adenine is now evident, although less intense than that of adenine over Si. The WF of the $PtNP_{UPW}$, increased with respect to that of the contaminated PtNPs, is now a little higher than the energy of the incident laser photons, and this suggested that the WF was sufficiently high to avoid the complete modification/destruction of adenine molecules.

The WF of the PtNPs could also be further increased for example by "doping" the nanoparticle with F (32, 35). HF was used to obtain such a doping ($PtNP_F$) starting from pure water $PtNP_{UPW}$ (Materials and Methods). The TEM measurements and the size distribution of the $PtNPs_F$ is reported in Fig. S3.

The XPS data showed a weak feature at about 687 eV (Fig. 6(C), green line) for F1s, which suggested that the amount of F atoms is low.

However, the UPS spectrum (Fig. 7, green line) showed a clear increase to 5.6 eV of the WF, a much higher value than the energy of the photons at 266 nm (4.66 eV). The low concentration of F could also suggest that the increase of the WF could be due to a "cleaning" effect of HF on $PtNP_F$. This is supported by the increase of the average diameter of the $PtNP_F$ (Fig. S3) to 20.5 nm, with respect to 13.8 nm for Na contaminated PtNPs and 12.5 nm for pure $PtNPs_{UPW}$. This increase suggested that this is a consequence of an Ostwald ripening effect in the laser ablation synthesis in which the smallest Pt particles are dissolved by HF and are redeposited on larger particles.

Using the same experimental protocol used for the first DUV SERS measurements we recorded the spectrum of adenine deposited on $PtNP_F$ as reported in Fig. 5(C). The peaks intensities now become similar to that of adenine over Si slide (Fig. 5(A)), showing that the increased WF of the particles allowed recovering the spectrum of adenine but with no appreciable SERS amplification.

PtNP diameter (nm) for NP in dimers (distance d between the NP (nm))	Largest SERS enhancement factor at 266 nm (4.66 eV)
10-10 (0)	$4.5\ 10^3$
10-10 (0.25)	$5.1\ 10^3$
20-20 (0)	$5.5\ 10^3$
20-20 (0.25)	$7.5\ 10^3$
30-30 (0)	$4.7\ 10^3$
30-30 (0.25)	$6.5\ 10^3$
50-50 (0)	$1.5\ 10^3$
50-50 (0.25)	$1.5\ 10^3$

Table 3. Largest calculated electromagnetic field SERS enhancements factors for Pt dimers as function of NPs diameters and distance. (($|E_{loc}(\omega_0)|/|$

$E_0(\omega_0)|)^4$, where E_{loc} is the local electric field found in the hot spot and E_0 is the applied electric field at ω_0) for dimers of PtNP, exciting at 266 nm (4.66 eV) in water with sizes ranging from 10 to 50 nm and distances between the NP d=0 nm and 0.25 nm.

The calculated hot spot SERS enhancements of dimers with 266 nm (4.66 eV) laser excitation are of the order of 10^3 (Table 3) however, experimentally there was not evident augmented peaks intensities of "millimolar adenine" on Pt NPs respect that on Si substrate. The absence of clear adenine plasmonic peaks enhancement using differently prepared Pt nanoparticles as SERS substrate in DUV makes possible to understand the role played by WF in DUV excited SERS experiments. These results allow concluding that the WF of the nanoparticles is a key parameter to consider for SERS experiments in the DUV.

WF can be the failure major cause in literature reported experimental studies on DUV SERS. In the literature experiments no one measured the WF of nanoparticles, nor XPS surveys, which guides to the interpretation of data and suggested us its tailoring. We note that in the case of the first reported study on UV-SERS of adenine using PtNPs (11), incident laser photons were at 325 nm (3.8 eV), a little above the WF found here for the Na contaminated PtNPs. Clearly, the WF of the PtNPs depends on the nanoparticles synthesis then on their surface "functionalization". However, in the above-mentioned study the lower energy of the photons suggests that the photoelectron extraction was not favored. In another literature case molecules of melanine were used for the DUV SERS experiments with DUV excitation at 244 nm (5.08 eV), (12). The LSPR were not identified for all the NP, but salts were used as SERS "activators" which could modify the WF of the PtNPs. The environment of the NP was, in this case, more complex than in other situations.(moreno, non capisco esattamente cosa intendi dire in questa frase) Clearly, measurements of the WFs of nanoparticles used for SERS experiments would be of interest to understand experimental results.

Other SERS experiments with PtNPs were obtained with visible or NIR exciting photons (13, 14) and, therefore photons had not enough energy to produce photoelectron extractions from the metal nanoparticles.

It is common to justify no appreciable experimental DUV SERS enhancement with Pt nanostructures, or to be precise no signal detection at all, with the presence of Pt interband transitions in this energy region of excitation. It is not trivial to extract precisely interband transition energies from experimental bands diagram of fcc Pt (25) or from PtNPs extinction spectra, experimental and calculated from dielectric functions data. It looks like, as a first approximation that in all the examined spectral region (200-1200 nm) interbands transitions gave their contribution in suppressing the plasmonic enhancement, and another focused research study is in progress.

Discussion

DUV excitation of LSPR in suitable metal nanostructures/nanoparticles to obtain SERS of molecules in traces is and was an ambitious research objective for the peculiarities open by DUV spectral region excitation: intense signals, fluorescence free SERS spectra, possible resonance coupling particularly interesting for the study of biological molecules (SERRS-surface enhanced resonant Raman scattering), the latter offering further signal enhancement of some orders of magnitude, respect to the pure SERS effect. The maximum reported enhancement with Au NPs with visible excitation of LSPR with SERRS effect was of 10^{15}, pushing the molecules detection limit in the femtomolar region (36). In DUV a similar and better effect was expected at the beginning of the researchers' investigations. Here, as a starting point it was chosen to analyze how Pt nanoparticles, stable in demanding environments, can be used for DUV SERS. The here developed methodology answers to literature requests of exploitation DUV SERS experiments. Here performed classical Mie electrodynamics calculations with comparative testing of experimental dataset for the metal dielectric function have shown that in the DUV region input field enhancement factors with PtNPs are not high also for aggregates with several hot spots. Moreover, DUV SERS experiments showed an unexpected failure in obtaining the spectrum of a molecule like adenine over PtNPs: this was rationalized and interpreted by measuring the WF of the Pt nanostructures. Modification/tuning of PtNPs WF allows to affirm that such a parameter would be determinant for metal SERS substrates in DUV region where ionization of the analyte and its destruction at metal surface follows from electron ejection and bombardment here of adenine. It is probable that the failure of many DUV SERS experiments reported in the literature, also with other nanometric plasmonic metals, has to be traced back to their WF, native (about 5 eV) or modified by surface contamination or surface modification. This phenomenon is not present in the visible and NIR regions, where most of the SERS experiments are usually performed, because excitation photon energies are sufficiently low compared to the WF. Measurement and eventually the tuning of the WF of the metal plasmonic substrates is therefore mandatory for DUV SERS experiments.

Materials and Methods

The Materials and Methods section should provide sufficient information to allow replication of the results. Begin with a section titled Experimental Design describing the objectives and design of the study as well as prespecified components.

Experimental Design

The original objective of the investigation was to obtain DUV SERS with naked PtNPs prepared by laser ablation in water for the detection of molecules in traces. The subject sounded interesting because in the past two decades results were poor and unclear in spite of promises based on few spare and maybe fortunate results, by chance obtained, as described in the introduction. Literature predictions based on

optical functions were (Fernando..) favourable for plasmonics in DUV. The design of the research study needed first of all to synthesize the NPs, to characterize them for optical properties, morphology, crystallographic structure, surface composition and properties, then finally to perform DUV SERS with the choice of a molecule in the detection of which there is an interest. In the present research study there was a deviation from the linear process in some sense, because at first no DUV SERS with adenine was obtained, and it was necessary to investigate NPs properties deeply and to find that WF was the important parameter to modify to obtain DUV SERS.

Chemicals

Adenine powder, Pt metal wire, Ultrapure Water (Certipur Conductivity water, nominal 0 mS/cm) and HF 40% solution were purchased from Sigma Aldrich, doubly distilled water was produced in the electrochemical lab of the Chemical Science Department at University of Padova.

NPs synthesis

Laser ablation syntheses in solution of PtNPs were produced with a pure Pt target under water (double distilled for PtNPs and normal glassware for the first experiment where Na contamination was found, then at a second stage Certipur Conductivity water for $PtNP_{UPW}$ and quartz glassware) using 1064 nm laser line in pulses of 8 ns at repetition rate of 20 Hz (Quantel Nd:YAG laser). The fluence was 4 J/cm^2 on the target. The Pt target was irradiated for 30 min changing continuously the incidence point at the laser focus on the target. $PtNP_F$ (fluorine doped) were prepared by processing $PtNP_{UPW}$ with a solution of HF at a final concentration of 4 % for half an hour at room temperature. Nanoparticles were then washed centrifuged and resuspended in ultrapure water until pH neutrality.

Extinction spectra

Extinction spectra of suspended nanoparticles in water medium and adenine in EtOH were recorded with a Cary 5000 (Agilent Technologies) spectrometer using 2 mm quartz cuvettes with solvent baseline correction in a single ray mode.

Morphological analysis

Low resolution TEM measurements were performed at the Biology Department of Università degli Studi di Padova with FEI Tecnai G12 electronic microscope. The copper grid entered in a low coat discharge machine, then a micro drop of the NPs suspension was deposited and dried. Statistics on NPs were performed with the free software ImageJ in manual mode on about 400 particles. Distributions fitting were performed with Igor 9 (Wavemetrics Corporation).

Crystallographic analysis

XRD was performed D8-Discover Bruker diffractometer. equipped with a Cu source (operated at 40/40 mA/kV), a Goebel mirror, a Eulerian cradle goniometer, and a scintillator detector. The sample of Pt NPs was deposited by successive drop casting on Si100 at about 100°C on a heating plate, allowing the solvent to evaporate. XRD patterns were collected, in 2θ scan mode with a fixed incident angle of 3°, moving the detector over the 2θ range 20°– 120° with a step size of 0.05°. A qualitative analysis of the crystalline phase content was performed using the QUALX 2.0 program (37).

Surface analysis

XPS measurements were performed at Analytical Laboratory of CNR-IOM in Basovizza (TS) with a hemispherical electron energy analyser, and a conventional Mg X-ray source with an overall energy resolution of 0.8 eV. The Pt NPs suspension were successively drop casted on Si 100. Spectra for Pt nanoparticles film is first acquired at room temperature, then sample is annealed at 250 °C for 5 min maintaining the base pressure of the chamber to 8 x 10^{-9} mbar. After 5 min sample is cooled and spectra is recorded. Similarly, Spectra for Polycrystalline Pt film, prepared for comparison by sputtering, was recorded before and after thermal annealing. Sputtering was done Argon at 2KV energy for 30 min. All the spectra recorded were calibrated by fixing the C1s peak of contaminants to 284.6 eV (not shown here). Analysis of XPS spectra were done by performing a non-linear mean square fit of the data, supposing that each component should have a Doniach-Siunich line shape superimposed to a Shirley background, and the shift between the incident radiation energy and Fermi energy is recorded.

Computational analysis

The Boundary Element Method (BEM) approach was used for solving the Maxwell equations for Mie scattering problem allowing the calculations of extinction spectra of PtNPs and SERS field enhancement factors. The computation used a MATLAB platform and the toolbox MNPBEM (22). Calculations were performed at Cloud Veneto infrastructure (cloudveneto.it).

SERS analysis

DUV SERS measurements were performed at the IUVS beamline laboratory of Elettra Sincrotrone di Trieste. A complete description of the experimental apparatus can be found elsewhere (38). SERS spectra were recorded exciting at 266 nm with 200 μW focused on the sample with a 100 mm plano-convex lens. Scattered photons were collected in a backscattering configuration. A Czerny-Turner spectrometer with focal length of 750 mm, coupled with a holographic reflection grating of 1800 g/mm and with a Peltier-cooled back-thinned

CCD was employed to get the Raman signal. Spectral resolution was set to 8 cm^{-1}. Raman frequencies were calibrated by means of cyclohexane spectra (39).

Supplementary material

This pdf file includes:

Fig. S1-S7

Extended Acknowledgements

References

1. B. Ren, X. Yang, Z., G. Liu, R. Aroca, B. Mao, Z. Tian, Surface-enhanced Raman scattering in the ultraviolet spectral region: UV-SERS on rhodium and ruthenium electrodes. *Journal of The American Chemical Society*, **125** (32), 9598-9599, (2003).

2. T. Dörfer, M. Schmitt, J. Popp, Deep-UV surface-enhanced Raman scattering. *Journal of Raman Spectroscopy*, **38** (11), 1379-1382, (2007).

3. B. Sharma, M. Cardinal, M. Ross, A. Zrimsek, S. Bykov, D. Punihaole, S. Asher, G. Schatz, R. Van Duyne, Aluminum Film-Over-Nanosphere Substrates for Deep-UV Surface-Enhanced Resonance Raman Spectroscopy. *Nano Letters*, **16** (12), 7968-7973, (2016).

4. J. Yi, E. You, R. Hu, D. Wu, G. Liu, Z. Yang, H. Zhang, Y. Gu, Y. Wang, X. Wang, et al. Surface-enhanced Raman spectroscopy: a half-century historical perspective. *Chemical Society Reviews*, **54** (3), 1453-1551, (2025).

5. H. Braddick, W. Tipping, E. Grant, N. Tomkinson, K. Faulds, D. Graham, Emerging applications of stimulated Raman scattering microscopy for medicinal chemistry and drug discovery. *Chemical Society Reviews*, *54* (23), 11266-11301, (2025).

6. M. M. H. Kneipp, H. Kneipp. *Surface-Enhanced Raman Scattering*; Springer-Verlag, (2006).

7. E. Le Ru, P. Etchegoin, *Principles of Surface-Enhanced Raman Spectroscopy and related plasmonic effects*; Elsevier Science, (2009).

8. S.; Nie, S. R. Emory, Probing single molecules and single nanoparticles by surface-enhanced Raman scattering. *Science*, **275** (5303), 1102-1106, (1997).

9. M. Knight, N. King, L. Liu, H. Everitt, P. Nordlander, N. Halas, Aluminum for Plasmonics. *ACS Nano*, **8** (1), 834-840, (2014).

10. F. Bisio, R. Proietti Zaccaria, R. Moroni, G. Maidecchi, A. Alabastri, G. Gonella, A. Giglia, L. Andolfi, S. Nannarone, L. Matera, M. Canepa, Pushing the high energy limit of Plasmonics, *ACS Nano*, **8**, 9239-9247, (2014).

11. L. Cui, A. Wang, D. Wu, B. Ren, Z. Tian, Shaping and Shelling Pt and Pd Nanoparticles Ultraviolet Laser Excited Surface-Enhanced Raman Scattering. *Journal of Physical Chemistry C*, **112** (45), 17618-17624, (2008).

12. E. Kämmer, T. Dörfer, A. Csáki, W. Schumacher, P. Da Costa, N. Tarcea, W. Fritzsche, P. Rösch, M. Schmitt, J. Popp, Evaluation of Colloids and Activation Agents for Determination of Melamine Using UV-SERS. *Journal of Physical Chemistry C*, **116** (10), 6083-6091, (2012).

13. M. Abdelsalam, S. Mahajan, P. Bartlett, J. Baumberg, A. Russell, SERS at structured palladium and platinum surfaces. *Journal of The American Chemical Society*, **129** (23), 7399-7406, (2007).

14. K. Kim, H. Lee, J. Choi, K. Kim, K. Shin, Surface-Enhanced Raman Scattering of 4-Aminobenzenethiol in Nanogaps between a Planar Ag Substrate and Pt Nanoparticles. *Journal of Physical Chemistry C*, **115** (27), 13223-13231, (2011).

15. V. Amendola, M. Meneghetti, Controlled size manipulation of free gold nanoparticles by laser irradiation and their facile bioconjugation. *Journal of Materials Chemistry*, **17** (44), 4705-4710, (2007).

16. M. Meneghetti, A. Scarsi, L. Litti, G. Marcolongo, V. Amendola, M. Gobbo, M. Di Chio, A. Boscaini, G. Fracasso, M. Colombatti, Plasmonic Nanostructures for SERRS Multiplexed Identification of Tumor-Associated Antigens. *Small*, **8** (24), 3733-3738, (2012).

17. F. Bertorelle, M. Pinto, R. Zappon, R. Pilot, L. Litti, S. Fiameni, G. Conti, M. Gobbo, G. Toffoli, M. Colombatti, et al. Safe core-satellite magneto-plasmonic nanostructures for efficient targeting and photothermal treatment of tumor cells. *Nanoscale*, **10** (3), 976-984, (2018).

18. F. Biscaglia, S. Rajendran, P. Conflitti, C. Benna, R. Sommaggio, L. Litti, S. Mocellin, G. Bocchinfuso, A. Rosato, A. Palleschi, et al. Enhanced EGFR Targeting Activity of Plasmonic Nanostructures with Engineered GE11 Peptide. *Advanced Healthcare Materials*, **6** (23), 1700596, (2017).

19. L. Litti, A. Colusso, M. Pinto, E. Ruli, A. Scarsi, L. Ventura, G. Toffoli, M. Colombatti, G. Fracasso, M. Meneghetti, SERRS multiplexing with multivalent nanostructures for the identification and enumeration of epithelial and mesenchymal cells. *Scientific Reports*, **10** (1), 15805, (2020).

20. M. Gobbo, I. Caligiuri, M. Giannetti, L. Litti, C. Mazzuca, F. Rizzolio, A. Palleschi, M. Meneghetti, SERS nanostructures with engineered active peptides against an immune checkpoint protein. *Nanoscale*, **16** (10), 5206-5214, (2024).

21. F. de Abajo, A. Howie, Retarded field calculation of electron energy loss in inhomogeneous dielectrics, 115418. *Physical Review B*, **65** (11), (2002).

22. U. Hohenester, Making simulations with the MNPBEM toolbox big: Hierarchical matrices and iterative solvers. *Computer Physics Communications*, **222**, 209-228, (2018).

23. A. Tselin, M. Pogodaeva, S. Levchenko, A. Kalmykov, K. Garbuzov, A. Smirnov, V. Drachev, Exploring the dielectric function of platinum. *Physical Review B*, **110** (19), (2024).

24. G. Mie, *Ann. Phys.* **25**, 337 (1908).

25. J. H. Weaver, Optical properties of Rh, Pd, Ir, and Pt. *Phys. Rev. B* **11**, 1416 (1975).

26. M. N. Polyanskiy. Refractiveindex.info database of optical constants. *Sci. Data,* **11**, 94 (2024).

27. E. Le Ru, B. Auguié, Enhancement Factors: A Central Concept during 50 Years of Surface-Enhanced Raman Spectroscopy. *ACS Nano*, **18** (14), 9773-9783, (2024).

28. L. Litti, M. Meneghetti, Predictions on the SERS enhancement factor of gold nanosphere aggregate samples. *Physical Chemistry Chemical Physics*, **21** (28), 15515-15522, (2019).

29. R. Esteban, A. Borisov, P. Nordlander, J. Aizpurua, Bridging quantum and classical plasmonics with a quantum-corrected model. *Nature Communications*, **3**, 825, (2012).

30. U. Hohenester, Quantum corrected model for plasmonic nanoparticles: A boundary element method implementation. *Physical Review B*, **91** (20), (2015).

31. M. Salmeron, S. Ferrer, M. Jazzar, G. A. Somorjai, Photoelectron-spectroscopy study of the electronic structure of Au and Ag overlayers on Pt(100), Pt(111), and Pt(997) surfaces. *Physical Review B*, **28** (12), 8, (1983).

32. A. Zangwill, *Physics at Surfaces*; Cambridge University Press, (1989).

33. G. Derry, M. Kern, E. Worth, Recommended values of clean metal surface work functions. *Journal of Vacuum Science & Technology A*, **33** (6), (2015).

34. S. Denifl, P. Sulzer, A. Mauracher, M. Probst, T. Märk, P. Scheier, Site selective cleavage of purine derivatives by capture of low energy electrons. *Physica Scripta*, **78** (5), (2008).

35. F. Gossenberger, T. Roman, K. Forster-Tonigold, A. Gross, Change of the work function of platinum electrodes induced by halide adsorption. *Beilstein Journal of Nanotechnology*, **5**, 152-161, (2014).

36. S. Schlücker, Surface-Enhanced Raman Spectroscopy: Concepts and Chemical Applications. *Angew. Chem. Int. Ed.* **53**, 2, (2014).

37. A. C. Altomare, C. Cuocci, A. Falcicchio, A. Moliteni, R. Rizzi, Qualitative phase analysis software using freely available database POW_COD., *J. Appl. Cystallogr.* 48, 598, (2015).

38. F. D'Amico, S. M. Bencivenga, M. Marsi, A. Gessini, G. Camisasca, E. Principi, R. Cucini, Di facility at Elettra. *Nuclear Instruments and Methods in Physics Research Section A: Accelerators, Spectrometers, Detectors and Associated Equipment* 703, 33, (2013).

39. R. L. McCreery, *Handbook of Vibrational Spectroscopy Vol. 1*, ed. J. M. Chalmers and P. R. Griffiths, Wiley, (2006).

Supplementary Materials References

40. M. Peukert, H. Bonzel, Characterization of oxidized Platinum surfaces by X-Ray Photoelectron Spectroscopy *Surface Science* **145**, 239-259 (1984).

41. J. S. Hammond, N. Winograd, XPS spectroscopic study of potentiostatic and galvanostatic oxidation of Pt electrodes in H2SO4

and HClO4. *Journal of Electroanalytical Chemistry and Interfacial Electrochemistry* **78**, 55-69 (1977).
42. H. T. Masami Taguchi, S. Nakajima. Methanol Oxidation Activity and Chemical State of Platinum Oxide Thin Film Treated by Electrochemical Reduction. *Materials Transactions* **54**, 582-587 (2013).
43. M. G. Z. Rondelli, M. Krause, M. D. Rötzer, M. N. Hedhili, M. P. Högerl, V. D'Elia, F. F. Schweinberger, J. M. Basset, U. Heiz. Exploring the Potential of Different-Sized Supported Subnanometer Pt Clusters as Catalysts for Wet Chemical Applications. *ACS Catal.* **7**, 4152-4162 (2017).
44. F. Mafunè, J-Y Khono, Y. Takeda, T. Kondow, Formation of stable platinum nanoparticles by laser ablation in water. *The Journal of Physical Chemistry B* **107**, 4218, (2003).
45. W. T. Nichols, N. Koshizaki, Laser ablation of a platinum target in water. III. Laser induced reactions. *Journal of Applied Physics* **100**, 114913, (2006).

Acknowledgments

We would like to thank C. Giannini and T. Sibillano, for checking the crystallographic structure and phases of PtNPs; A. Tselin, I. M. Doludenko, S. A. Bedin for checking the crystallographic structure of their target; S. Bardwaj for help in XPS-UPS measurements, S. Modesti G. Panaccione and G. M. Pirantozzi for discussions about EELS datasets and interband transitions in Pt; S. Rubini and L. Manna for discussing PtNPs crystallinity; R. Ciancio and D. Knez for HRTEM measurements on Pt NPs; B. Rossi for help in preparation of CERIC-ERIC proposal for IUVS laboratory at Elettra.

Funding: Include all funding sources, including grant numbers, complete funding agency names, and recipient's initials. Each funding source should be listed in a separate paragraph such as:

CERIC-ERIC grant, BFS, MM
IOM -CNR fundings, BFS
University of Padova fundings, MM
Infrastructures: IOM-CNR, University of Padova, Elettra Sincrotrone di Trieste

National Institutes of Health grant U12AV123456 (PV, CHO)
National Institutes of Health grant R01AB123456 (PV, GS)
William K. Bowes Jr Foundation (PV)
German Research Foundation grant AB 1234/1-1
Office of Biological and Environmental Research of the U.S. Department of Energy Atmospheric System Research Program Interagency Agreement grant DE-SC0000001
National Institute of Health Researh UK

Author contributions:
Examples:
Conceptualization: MM

Methodology: BFS, MM, AM, CC, FDA
Investigation: BFS, MM/calculations; CC, AM/XPS-UPS, FDA/DUV SERS
Visualization: BFS, MM, AM, CC, FDA
Supervision: MM, AM
Writing—original draft: BFS, MM, AM, CC, FDA
Writing—review & editing: BFS, MM
Fundings: MM, AM

Competing interests:
Authors declare that they have no competing interests.

Supplementary Materials

Fig. S1-S7
Extended Acknowledgements